Syntheses, crystal structures, and resistivities of the two new ternary uranium selenides, Er_3USe_8 and Yb_3USe_8

Jai Prakash[a], Adel Mesbah[a,b], Jessica C. Beard[a], Christos D. Malliakas[a], and James A. Ibers[a,*]

[a]Department of Chemistry, Northwestern University, 2145 Sheridan Road, Evanston, IL 60208-3113, United States.

[b]ICSM, UMR 5257 CEA / CNRS / UM2 / ENSCM, Site de Marcoule - Bât. 426, BP 17171, 30207 Bagnols-sur-Cèze cedex, France.

Keywords: lanthanide uranium selenides; crystal structure; resistivity

Abstract

Two new ternary lanthanide (Ln) uranium selenides, Er_3USe_8 and Yb_3USe_8, were synthesized at 1198 K using NaI as a flux. Single-crystal X-ray studies show these two compounds to be isostructural and to crystallize in space group D_{2h}^{11}-*Pbcm* of the orthorhombic crystal system. The Ln and U atoms are disordered on the same crystallographic site in these crystal structures. Each Ln/U atom is coordinated to eight Se atoms in a bicapped trigonal prism, and sharing of these $(Ln/U)Se_8$ units creates a three-dimensional network. Se2 atoms are connected to each other to form infinite one-dimensional chains along the *c* axis. In these chains, the two Se atoms are separated by about 2.74 Å, a distance intermediate to those of a Se−Se single bond and a van der Waals interaction. Temperature-dependent resistivity measurements show that Er_3USe_8 and Yb_3USe_8 are semiconductors with activation energies of 0.08(1) and 0.17(1) eV, respectively.

*Corresponding author.

E-mail address: ibers@chem.northwestern.edu (J.A.Ibers)

1. Introduction

One of the major challenges in the processing of nuclear waste is the separation of radioactive An^{3+} species from Ln^{3+} species (An = actinide; Ln = lanthanide) because of their similar ionic sizes and chemistry. To develop an effective method for separation of these species, research has focused on their solution chemistry [1-3]. However, the chemistry of actinides and lanthanides in solid-state compounds is less studied and somewhat neglected as compared with their solution chemistry. The crystal structures of most of the extended solid-state compounds either show disorder between Ln and An or are an ordered variant of their known binary phases. Examples of compounds whose structures show Ln/An disorder include $(Ln/Th)O_2$ (Ln = La, Nd, Sm, Gd) [4], (Ln/U)N (Ln = La-Nd, Sm, Gd, Dy, Er) [5], $(Ln/U)_3Q_4$ (Ln = La, Ce, Pr; Q = S, Se, Te) [6], (Ln/U)S (Ln = Pr, Nd) [7], and $(Ln/U)Te_3$ (Ln = La-Nd, Sm, Gd-Lu) [8,9]. Examples of compounds in whose structures Ln and An atoms occupy different crystallographic sites are $(Ln^{3+})_2An^{4+}Q_5$ (Ln = La-Gd, Q = S, Se) [10-12] and $(Ln^{3+})_6(U^{6+})O_{12}$ (Ln = La, Lu) [13]; these are ordered variants of the structures of the binary compounds U_3S_5 [14] and Ln_7O_{12} [15], respectively.

There are only a few structures of solid-state compounds where An and Ln atoms occupy different crystallographic sites in new structure types as well. These include $Cs_{11}Eu_4(UO_2)_2(P_2O_7)_6(PO_4)$ [16], $Nd[(UO_2)_3O(OH)(PO_4)_2]\bullet 6H_2O$ [17], $H_2[Nd_2(H_2O)_{12}UMo_{12}O_{42}]\bullet 12H_2O$ [18], $Ln_3UO_6Cl_3$ (Ln = La, Pr, Nd) [19], $EuUI_6$ [20], and $La_2U_2Se_9$ [21], the last being the only example of an Ln/An chalcogenide.

In order to extend the solid-state chemistry of Ln/An compounds we have carried out exploratory syntheses in the Ln/U/Se system. Our efforts have led to discovery of the two new isostructural compounds Er_3USe_8 and Yb_3USe_8. Though the structure of these compounds shows Ln/U disorder it is not a variant of a known binary structure. Here we present the syntheses, crystal structures, and electrical properties of Er_3USe_8 and Yb_3USe_8.

2. Experimental

2.1 Syntheses

Caution! Depleted U is an α-emitting radioisotope and as such is considered a health risk. Its use requires appropriate infrastructure and personnel trained in the handling of radioactive materials.

The starting materials, Yb (Alfa, 99.9 %), Er (Alfa, 99.9 %), NaI (Alfa, 99.5%), and Se (Cerac, 99.999 %) were used as obtained. Depleted U powder was obtained by hydridization and decomposition of U turnings (IBI Labs) in a modification [22] of a previous literature method [23]. Reactions were performed in sealed 6 mm carbon-coated fused-silica tubes. Chemical manipulations were performed inside an Ar-filled dry box. The reactants were weighed and transferred into tubes that were then evacuated to 10^{-4} Torr, flame sealed, and heated in a computer-controlled furnace.

Semi-quantitative EDX analyses of the products of the reactions were obtained with the use of a Hitachi S-3400 SEM microscope. The EDX analyses of the desired products were repeated from crystal to crystal and the results were Ln:U = 3:1 with a 5% deviation. Unit cells of several of these Ln_3USe_8 crystals that had been attached to carbon tape for EDX analysis did not show significant variations in cell constants. In each instance from among those crystals one was selected for the X-ray structure determination.

Synthesis of Er_3USe_8. Crystals of Er_3USe_8 were obtained by the reaction of elements Er (14.0 mg, 0.0837 mmol), U (10 mg, 0.0420 mmol), Se (33.2 mg, 0.4205 mmol), with excess NaI flux (58.0 mg, 0.387 mmol). The reaction mixture was heated to 1053 K at 33 K/h, held there for 24 h, heated to 1198 K at 6 K/h, held there for 99 h, cooled to 998 K at 2 K/h, to 598 K at 4 K/h, and then to 298 K at 12.5 K/h. The reaction product was washed with acetone to remove the NaI flux and then dried under vacuum for 2 h. The washed product contained black plates and needles of Er_3USe_8 (Er:U:Se ≈ 3:1:8), Er_2Se_3 [24] (Er:Se ≈ 2:3), and black plates of UOSe (U:Se ≈ 1:1) [25].

Synthesis of Yb_3USe_8. Crystals of Yb_3USe_8 were obtained by the reaction of elements Yb (14.5 mg, 0.0838 mmol), U (10 mg, 0.0420 mmol), Se (33.2 mg, 0.4205 mmol), with excess NaI flux (57.7 mg, 0.385 mmol). The same procedures as for Er_3USe_8 resulted in a washed product

that contained black plates and needles of Yb_3USe_8 (Yb:U:Se ≈ 3:1:8) along with Yb_2Se_3 [26] and UOSe [25].

2.2 Structure determinations

The crystal structures of Er_3USe_8 and Yb_3USe_8 were determined from single-crystal X-ray diffraction data collected with the use of graphite-monochromatized MoKα radiation (λ = 0.71073 Å) at 100(2) K on a Bruker APEX2 diffractometer [27]. The algorithm COSMO implemented in the program APEX2 was used to establish the data collection strategy with a series of 0.3° scans in ω and φ. The exposure time was 15 sec/frame and the crystal-to-detector distance was 50 mm for both compounds. The collection of intensity data as well as cell refinement and data reduction were carried out with the use of the program APEX2 [27]. Face-indexed absorption, incident beam, and decay corrections were performed with the use of the program SADABS [28]. Precession images of the data sets provided no evidence for supercells or modulations. The crystal structures of these two compounds were solved and refined with the use of the SHELX-14 algorithms of the SHELXL program package [28,29]. A disorder between Ln and U at the (4d) crystallographic site was observed for both compounds. Determination of chemical composition from X-ray diffraction data is fraught with difficulties under the best of circumstances. In the present instance a determination of the Ln:U ratio by refinement of their occupancies at this common site is out of the question because the very small cell volume precludes there being a sufficient number of low-angle reflections sensitive to the differences in the atomic scattering factors of the respective elements. Accordingly, the occupancies of Ln and U were fixed at 3:1 as found by EDX measurements. A disorder between Ln and U is not surprising as their ionic radii in eight-fold coordination environment are essentially equal: Er^{3+} (1.004 Å), Yb^{3+} (0.985 Å), and U^{4+} (1.00 Å) [30].

2.3 Resistivity measurements

Four-probe temperature-dependent resistivity data for Er_3USe_8 and Yb_3USe_8 were collected using a home-made resistivity apparatus equipped with a Keithley 2182 nanovoltmeter, a Keithley 236 source measure unit, and a high-temperature vacuum chamber controlled by a K-

20 MMR system. An *I-V* curve from 1×10^{-8} to -1×10^{-8} A with a step of 4×10^{-9} A was measured for each temperature point (from 300 to 500 K) and resistance was calculated from the slope of the plot. Data acquisition was controlled by custom-written software. Graphite paint (PELCO Isopropanol based graphite paint) was used for electrical contacts with copper wire of 0.025 mm thickness (Omega). The DC current was applied along an arbitrary direction on a single crystal with dimensions $0.16 \times 0.05 \times 0.05$ mm and $0.20 \times 0.09 \times 0.07$ mm for Er_3USe_8 and Yb_3USe_3, respectively.

3. Results

3.1 Syntheses

Black single crystals of the compounds Er_3USe_8 and Yb_3USe_8 were first obtained by reactions of the elements in NaI molten flux in yields of about 50 wt% (based on U) during our exploration of the ternary Ln-U-Se system. These compounds were synthesized in about the same yields from stoichiometric reactions of the elements in the NaI molten flux using the same temperature profile. No further attempts were made to maximize the yields. The relatively small black crystals of these compounds could not be separated from the black crystalline secondary by-products UOSe and Ln_2Se_3. Thus, the magnetic properties of these compounds were not investigated.

3.2 Crystal structures

Er_3USe_8 and Yb_3USe_8. These two isostructural compounds crystallize in a new structure type with one formula unit in space group D_{2h}^{11}–*Pbcm* of the orthorhombic crystal system. A general view of crystal structure of Ln_3USe_8 (Ln = Er and Yb) is shown in Fig. 1 and metrical data are presented in Tables 1 and 2 and in Supplementary information. The Ln and U atoms in this structure are disordered on the (4*d*) crystallographic site. The asymmetric unit of the structure comprises one Ln/U site (site symmetry ..*m*) and two Se sites (Se1 (..*m*) and Se2 (2..)). Each Ln/U

atom is coordinated to eight Se atoms (4 × Se1 and 4 × Se2) in a bicapped trigonal prism (Fig. 2). This (U/Ln)Se_8 unit is connected to other neighboring (U/Ln)Se_8 polyhedra by edge-, corner-, and face-sharing to form a three-dimensional network. The U−Se interatomic distances (2.7867(4) to 3.0248(2) Å) in these two compounds are typical for U^{4+}−Se interactions in related compounds (Table 3). Se2 atoms in this structure form linear infinite chains running along the *c* direction with Se2−Se2 interactions of ~2.74 Å. These Se2−Se2 interactions are intermediate in length to an Se−Se single bond (~2.35 Å) and a van der Waals interaction. There are two Se infinite chains in the unit cell. In each the Se−Se distances are constant. The Se−Se interactions in the structures of related compounds are also presented in Table 3. Note that in these related structures the Se−Se distances are not constant but alternate ...long-short-long.... However, the average Se−Se distances in these compounds are comparable with the corresponding distances in the Ln_3USe_8 structures (Table 3). Theoretical calculations have shown that linear infinite chains with equidistant p-block atoms are unstable [31] and hence should lead to modulated structures as are known for KTh_2Se_6 [32], TlU_2Se_6 [33], and $CsNp_2Se_6$ [33]. However, no modulation was observed for the present Ln_3USe_8 structures. Moreover, the displacement parameters of the Se atoms are well behaved (Supplementary information).

As discussed earlier, most LnAnSe structures either exhibit Ln/An disorder or are ordered variants of known actinide or lanthanide binary structures. However, the crystal structure of Ln_3USe_8 [i.e., $(Ln_{0.75}U_{0.25})Se_2$] is very different from the structures of the simple binaries USe_2 (α and β-form) [34,35] and $LnSe_2$ (Ln = Er [36] and Yb [37]). Interestingly, the structure of Ln_3USe_8 is related to that reported for the compound $HfFe_2Si_2$ [38]. A comparison of these two structures is shown in Fig. 4. The $HfFe_2Si_2$ structure can be obtained from the $Ln_{0.75}U_{0.25}Se_2$ structure by replacing Hf with (Ln/U), Si with Se, and filling the empty (4*d*) and (4*c*) sites by Fe atoms, as shown in Fig. 4. $HfFe_2Si_2$ also features linear infinite chains of Si atoms.

The structures of the ternary Ln_2USe_5 [10,11] family of compounds in the Ln/U/Se system are derived from the U_3S_5 [i.e.,$(U^{3+})_2U^{4+}(S^{2-})_5$ [14] structure by replacing the two U^{3+} ions by two Ln^{3+} ions. Only one compound, namely $La_2U_2Se_9$ [21], is known among Ln/An/Q compounds where the Ln and An atoms are ordered and form a completely new structure type. In contrast to

the structure of Ln_3USe_8, the $La_2U_2Se_9$ [21] structure contains nine-coordinate U atoms and eight- and ten-coordinated La atom and three distinct types of linear infinite Se chains with alternating Se−Se distances (2.712(3), 2.748(3); 2.803(3), 2.807(3); 2.796(3), 2.814(3) Å).

3.3 Oxidation states

The presence of Se−Se−Se chains in Ln_3USe_8 with intermediate interactions makes the assignment of oxidation states arbitrary. One way of achieving charge balance in Ln_3USe_8 is 3 × Ln^{3+}, 1 × U^{4+}, and 4 × Se^{2-}. This assignment leads to an average charge of −1.25 e^- on each of the remaining four Se atoms involved in the formation of the linear Se chains. Thus these Se atoms are reduced as compared with those in the Se−Se single-bonded Se_2^{2-}dimers. This can be understood by imagining a U_4Se_8 [i.e., USe_2] compound with the same structure as Ln_3USe_8 but without short Se−Se single bonds. This compound can be charge balanced as 4 × U^{4+} and 8 × Se^{2-}. Aliovalent substitution of Ln^{3+} for U^{4+} in this imaginary compound will lead to oxidation. Thus stability of the structure depends on the redox tendencies of U^{4+} to U^{4+}/U^{5+} or Se^{2-} to $Se^{(2-)+x}$. In eight coordination the ionic radius of U^{5+} of about 0.89 Å is significantly smaller than that of Er^{3+} (1.004 Å) or Yb^{3+} (0.985 Å) and thus oxidation of U^{4+} to U^{5+} is not favorable for the stability of this structure as both Ln and U occupy the same site. Thus oxidation of Se^{2-} to form the linear Se chains with intermediate distances is one way to stabilize this structure type. There are many examples of actinide chalcogenides containing infinite linear Q chains where average charge on Q is non-integer and intermediate to that of −1 in Se_2^{2-} and −2 in Se^{2-}. For example, the ATh_2Se_6 (A= K and Rb) compounds [32] also feature linear Se chains with an average charge of −1.25 e^-on each Se atom.

3.4 Resistivity studies

Fig. 4 shows that Er_3USe_8 and Yb_3USe_8 are semiconductors. Their resistivities at 298 K of about 16 ohm.cm for Er_3USe_8 and 1000 ohm.cm for Yb_3USe_8 decrease at 500 K to about 10 ohm.cm and 100 ohm.cm, respectively. The activation energy estimated by the Arrhenius plot (Fig. 5) is 0.17(1) eV for Yb_3USe_8. The Arrhenius plot for Er_3USe_8 (Fig. 5) is not linear

suggesting a complex thermal activation of carriers with activation energies between 0.02(1) eV and 0.08(1) eV.

4. Conclusions

Two new ternary lanthanide (Ln) uranium selenides, Er_3USe_8 and Yb_3USe_8, were synthesized at 1198 K in a NaI flux. These isostructural compounds crystallize in a new structure type in space group D_{2h}^{11}-*Pbcm* of the orthorhombic system. Though their structure shows Ln/U disorder it is not a variant of a known binary structure. The crystal structure consists of one Ln/U site and two Se sites. Each Ln/U atom in this structure is connected to four Se1 and four Se2 atoms to form a (Ln/U)Se_8 polyhedron with bicapped trigonal-prismatic geometry. A three-dimensional network structure is formed by face-, edge-, and corner-sharing of these (Ln/U)Se_8 units. Se2 atoms in these structures are connected to each other to form infinite one-dimensional chains along the *c* axis. In these chains, the two Se atoms are separated by a distance intermediate to those of a Se−Se single bond and a van der Waals interaction. One way of achieving charge balance in Ln_3USe_8 is 3 × Ln^{3+}, 1 × U^{4+}, and 4 × Se^{2-}. This assignment leads to an average charge of −1.25 e^- on each of the remaining four Se atoms involved in the formation of these linear Se chains. Temperature-dependent resistivity measurements show that these compounds are semiconductors with activation energies of 0.02(1) to 0.08(1) eV (Er_3USe_8) and 0.17(1) eV (Yb_3USe_8).

Acknowledgments

Use was made of the IMSERC X-ray Facility at Northwestern University, supported by the International Institute of Nanotechnology (IIN). C.D.M. was supported by the U.S. Department of Energy, Office of Basic Energy Sciences, under Contract No. DE-AC02-06CH11357.

Appendix A. Supplementary information

Supplementary data associated with this article can be found in the online version at http://dx.doi.org.....Crystallographic data in cif format for Er_3USe_8 and Yb_3USe_3 have been deposited with FIZ Karlsruhe as CSD numbers 430143 and 430144, respectively. These data may be obtained free of charge by contacting FIZ Karlsruhe at +497247808666 (fax) or crysdata@fiz-karlsruhe.de (email).

References

[1] F.W. Lewis, L.M. Harwood, M.J. Hudson, M.G.B. Drew, J.F. Desreux, G. Vidick, N. Bouslimani, G. Modolo, A. Wilden, M. Sypula, T.-H. Vu, J.-P. Simonin, J. Am. Chem. Soc. 133 (2011) 13093-13102.

[2] A.V. Gelis, G.J. Lumetta, Ind. Eng. Chem. Res. 53 (2014) 1624-1631.

[3] Z. Kolarik, Chem. Rev. 108 (2008) 4208-4252.

[4] G. Brauer, H. Gradinger, Z. Anorg. Allg. Chem. 276 (1954) 209-226.

[5] P. Ettmayer, J. Waldhart, A. Vendl, Monatsh. Chem. 110 (1979) 1109-1112.

[6] P. Demoncy, P. Khodadad, Ann. Chim. (Paris) 5 (1970) 341-356.

[7] R. Troc, Physica B+C 102 (1980) 233-236.

[8] V.K. Slovyanskikh, N.T. Kuznetsov, Russ. J. Inorg. Chem. (Transl. of Zh. Neorg. Khim.) 35 (1990) 447.

[9] V.K. Slovyanskikh, N.T. Kuznetsov, N.V. Gracheva, V.G. Kipiani, Russ. J. Inorg. Chem. (Transl. of Zh. Neorg. Khim.) 30 (1985) 1720-1721.

[10] V.K. Slovyanskikh, N.T. Kuznetsov, N.V. Gracheva, Russ. J. Inorg. Chem. (Transl. of Zh. Neorg. Khim.) 29 (1984) 960-961.

[11] H. Noël, J. Prigent, Physica B+C 102 (1980) 372-379.

[12] V. Tien, M. Guittard, J. Flahaut, N. Rodier, Mater. Res. Bull. 10 (1975) 547-554.

[13] Y. Hinatsu, N. Masaki, T. Fujino, J. Solid State Chem. 73 (1988) 567-571.

[14] M. Potel, R. Brochu, J. Padiou, D. Grandjean, C. R. Seances Acad. Sci., Ser. C 275 (1972) 1419-1421.

[15] N.C. Baenziger, H.A. Eick, H.S. Schuldt, L. Eyring, J. Am. Chem. Soc. 83 (1961) 2219-2223.

[16] A.B. Pobedina, A.B. Ilyukhin, Russ. J. Inorg. Chem. (Transl. of Zh. Neorg. Khim.) 42 (1997) 1006-1010.

[17] P. Piret, M. Deliens, J. Piret-Meunier, Bull. Soc. Fr. Mineral. Cristallogr. 111 (1988) 443-449.

[18] E.P. Samokhvalova, V.N. Molchanov, I.V. Tat'yanina, E.A. Torchenkova, Sov. J. Coord. Chem. (Engl. Transl.) 16 (1990) 683-687.

[19] G. Henche, K. Fiedler, R. Gruehn, Z. Anorg. Allg. Chem. 619 (1993) 77-87.

[20] H.P. Beck, F. Kühn, Z. Anorg. Allg. Chem. 621 (1995) 1659-1662.

[21] D.E. Bugaris, R. Copping, T. Tyliszczak, D.K. Shuh, J.A. Ibers, Inorg. Chem. 49 (2010) 2568-2575.

[22] D.E. Bugaris, J.A. Ibers, J. Solid State Chem. 181 (2008) 3189-3193.

[23] A.J.K. Haneveld, F. Jellinek, J. Less-Common Met. 18 (1969) 123-129.

[24] C.M. Fang, A. Meetsma, G.A. Wiegers, J. Alloys Compd. 218 (1995) 224-227.

[25] M.F. Mansuetto, S. Jobic, H.P. Ng, J.A. Ibers, Acta Crystallogr. Sect. C: Cryst. Struct. Commun. 49 (1993) 1584-1585.

[26] N.W. Tideswell, F.H. Kruse, J.D. McCullough, Acta Cryst. 10 (1957) 99-102.

[27] Bruker APEX2 Version 2009.5-1 Data Collection and Processing Software,, Bruker Analytical X-Ray Instruments, Inc., Madison, WI, USA, 2009.

[28] G.M. Sheldrick, SADABS, 2008. Department of Structural Chemistry, University of Göttingen, Göttingen, Germany

[29] G.M. Sheldrick, Acta Crystallogr. Sect. A: Found. Crystallogr. 64 (2008) 112-122.

[30] R.D. Shannon, Acta Crystallogr. Sect. A: Cryst. Phys. Diffr. Theor. Gen. Crystallogr. 32 (1976) 751-767.

[31] G.A. Papoian, R. Hoffmann, Angew. Chem., Int. Ed. Engl. 39 (2000) 2408-2448.

[32] K.-S. Choi, R. Patschke, S.J.L. Billinge, M.J. Waner, M. Dantus, M.G. Kanatzidis, J. Am. Chem. Soc. 120 (1998) 10706-10714.

[33] D.E. Bugaris, D.M. Wells, J. Yao, S. Skanthakumar, R.G. Haire, L. Soderholm, J.A. Ibers, Inorg. Chem. 49 (2010) 8381-8388.

[34] H.P. Beck, W. Dausch, J. Solid State Chem. 80 (1989) 32-39.

[35] H. Noël, M. Potel, R. Troc, L. Shlyk, J. Solid State Chem. 126 (1996) 22-26.

[36] R. Wang, H. Steinfink, Inorg. Chem. 6 (1967) 1685-1692.

[37] A.W. Webb, H.T. Hall, Inorg. Chem. 9 (1970) 843-847.

[38] Y.P. Yarmolyuk, L.A. Lysenko, E.I. Gladyshevskii, Kristallografiya 21 (1976) 829-831.

[39] A. Daoudi, M. Lamire, J.C. Levet, H. Noël, J. Solid State Chem. 123 (1996) 331-336.

[40] I. Ijjaali, K. Mitchell, F.Q. Huang, J.A. Ibers, J. Solid State Chem. 177 (2004) 257-261.

[41] B.C. Chan, Z. Hulvey, K.D. Abney, P.K. Dorhout, Inorg. Chem. 43 (2004) 2453-2455.

[42] H. Mizoguchi, D. Gray, F.Q. Huang, J.A. Ibers, Inorg. Chem. 45 (2006) 3307-3311.

[43] A. Daoudi, H. Noël, J. Alloys Compd. 233 (1996) 169-173.

[44] J. Prakash, M.S. Tarasenko, A. Mesbah, S. Lebègue, C.D. Malliakas, J.A. Ibers, Inorg. Chem. 53 (2014) 11626-11632.

Table 1. Crystallographic data and structure refinement details for Er_3USe_8 and Yb_3USe_8.[a]

	Er_3USe_8	Yb_3USe_8
a (Å)	7.0360(2)	6.9937(2)
b (Å)	7.5483(2)	7.4807(2)
c (Å)	5.4672(1)	5.4967(2)
V (Å^3)	290.36(1)	287.58(2)
ρ (g cm^{-3})	7.843	8.019
μ (mm^{-1})	60.366	63.455
$R(F)$[b]	0.009	0.013
$R_w(F_o^2)$[c]	0.021	0.032

[a] $\lambda = 0.71073$ Å, $Z = 1$, $T = 100(2)$ K, space group D_{2h}^{11}–$Pbcm$.

[b] $R(F) = \Sigma \left| \left| F_o \right| - \left| F_c \right| \right| / \Sigma \left| F_o \right|$ for $F_o^2 > 2\sigma(F_o^2)$.

[c] $R_w(F_o^2) = \{\Sigma [w(F_o^2 - F_c^2)^2] / \Sigma w F_o^4\}^{1/2}$. For $F_o^2 < 0$, $w^{-1} = \sigma^2(F_o^2)$; for $F_o^2 \geq 0$, $w^{-1} = \sigma^2(F_o^2) + (qF_o^2)^2$ where $q = 0.0110$ for Er_3USe_8 and 0.0094 for Yb_3USe_8

Table 2. Selected interatomic lengths (Å) for Er_3USe_8 and Yb_3USe_8.

	Er_3USe_8[a]	Yb_3USe_8[a]
Ln/U1−Se1	2.8016(3) × 1	2.7867(4) × 1
	2.8075(3) × 1	2.8018(4) × 1
	2.8952(1) × 2	2.9105(2) × 2
Ln/U1−Se2	2.9738(1) × 2	2.9498(2) × 2
	3.0248(2) × 2	3.0036(3) × 2
Se2•••Se2	2.7336(1) × 2	2.7484(1) × 2
U1/Ln1•••U1/Ln1	4.0163(2) × 2	4.0098(2) × 2

[a]Both Er or Yb and U occupy same crystallographic site (4*d*).

Table 3: U−Se and Se−Se interactions (Å) in some related compounds

Compound	Structure[a]	U−Se[b]	Se−Se	Reference
Er_3USe_8	3D	2.802(1)−3.025(1)	2.734(1)	this work
Yb_3USe_8	3D	2.787(1)−3.004(1)	2.748(1)	this work
$Cu_2U_3Se_7$	3D	2.766(1)−3.212(1)	-	[39]
$MnUSe_3$	3D	2.850(2)−3.126(3)	-	[40]
CsU_2Se_6	Layered	2.895(1)−2.960(1)	2.665(1), 2.894(1)	[41]
KU_2Se_6	Layered	2.888(1)−2.965(1)	2.703(1), 2.855(1)	[42]
RbU_2Se_6	Layered	2.891(1)−2.961(1)	2.698(1), 2.854(1)	[33]
TlU_2Se_6	Layered	2.884(1)−2.957(1)	2.704(1), 2.848(1)	[33]
$Rh_2U_6Se_{15.5}$	3D	2.866(1)−2.985(1)	-	[43]
BaU_2Se_5[a]	3D	2.858(1)−3.110(1)	-	[44]
$La_2U_2Se_9$	3D	2.892(1)−3.040(1)	2.712(3)− 2.814(3)	[21]

[a]In $La_2U_2Se_9$ each U atom is nine-coordinate in a monocapped square antiprism; in all the other structures each U atom is eight-coordinate in a bicapped trigonal prism.

[b]Some interatomic distances have been rounded to facilitate the comparisons.

Figure Legends.

Fig.1. Crystal structure of Ln_3USe_8 (Ln = Er, Yb) viewed along *c* axis. Se−Se interactions are shown as thick blue lines for clarity.

Fig.2. Local coordination environment of (*Ln*/U) atoms in the Ln_3USe_8 (*Ln* = Er, Yb) structure.

Fig. 3. Structural relationship between the Ln_3USe_8 (Ln = Er, Yb) and the $HfFe_2Si_2$ structures [38].

Fig.4. (Left) Temperature-dependent resistivities forEr_3USe_8 single crystals showing semiconducting behavior. (Right) Arrhenius plots.

Fig.5. (Left) Temperature-dependent resistivities forYb_3USe_8 single crystals showing semiconducting behavior. (Right) Arrhenius plots.

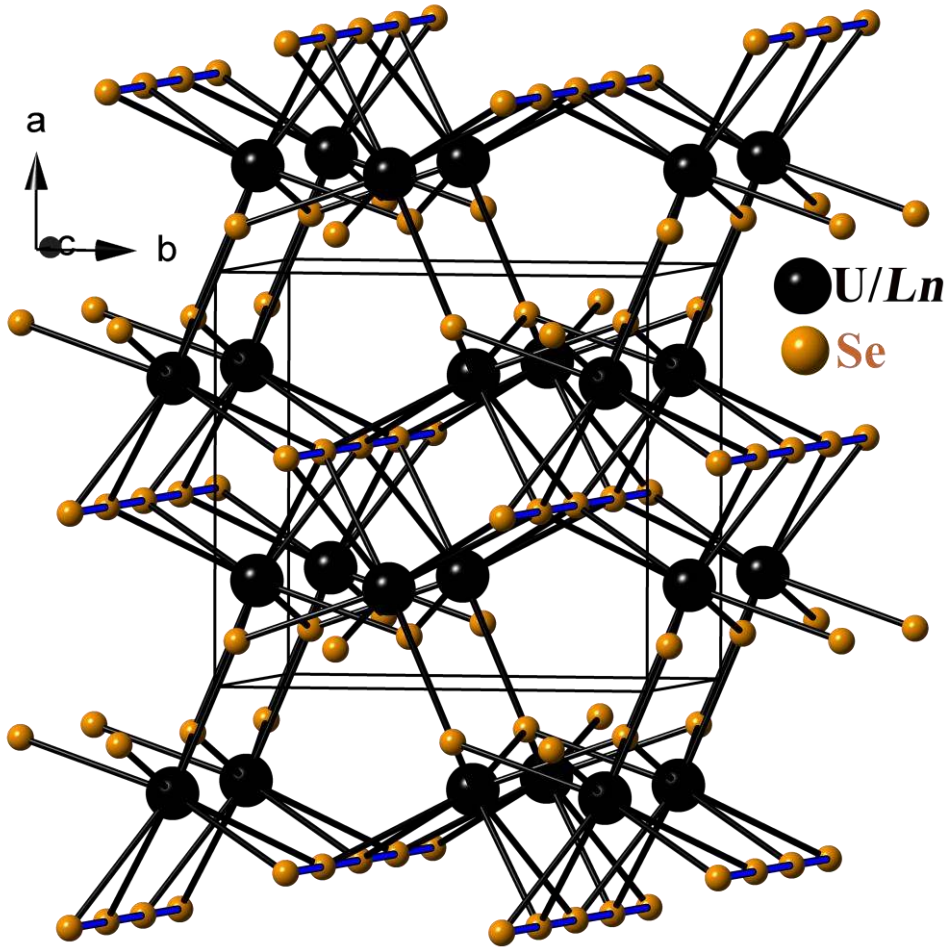
a
c
b
U/Ln
Se

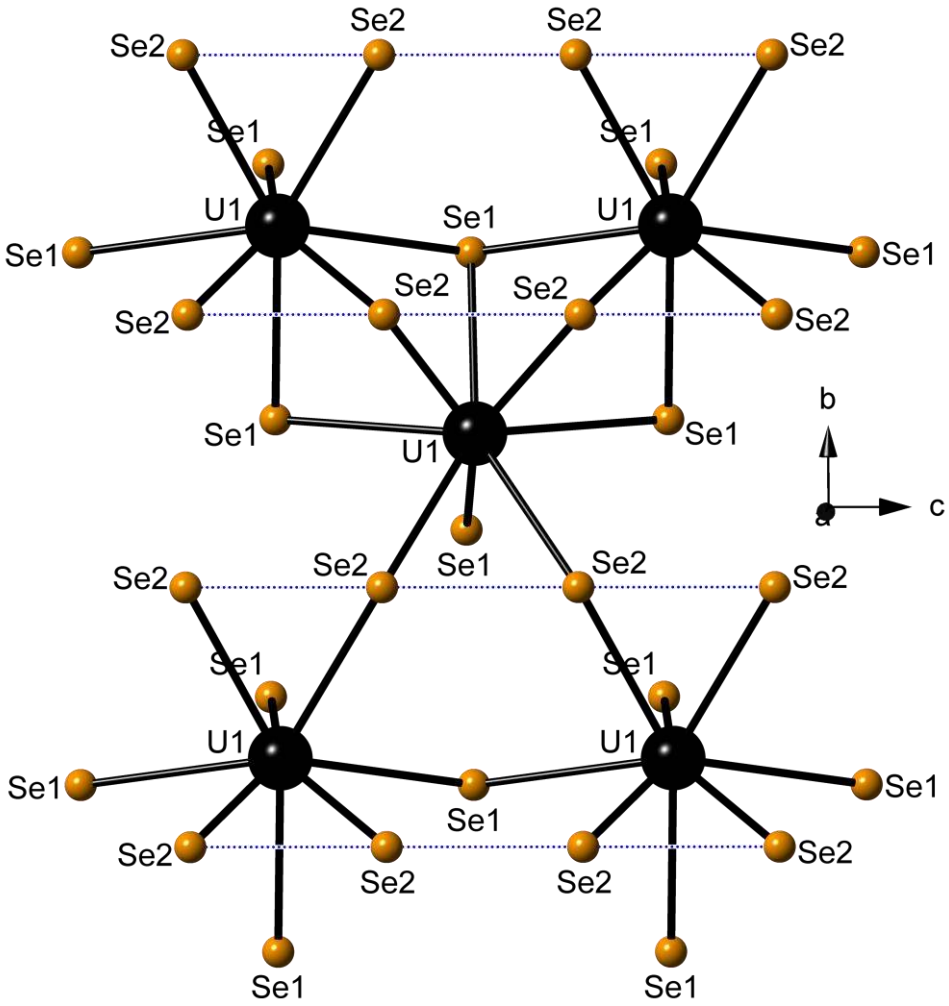
Se2
Se2
Se2
Se2
Se1
Se1
U1
Se1
U1
Se1
Se1
Se2
Se2
Se2
Se2
Se1
U1
Se1
b
c
a
Se2
Se2
Se1
Se2
Se2
Se1
Se1
U1
U1
Se1
Se1
Se2
Se2
Se2
Se2
Se1
Se1

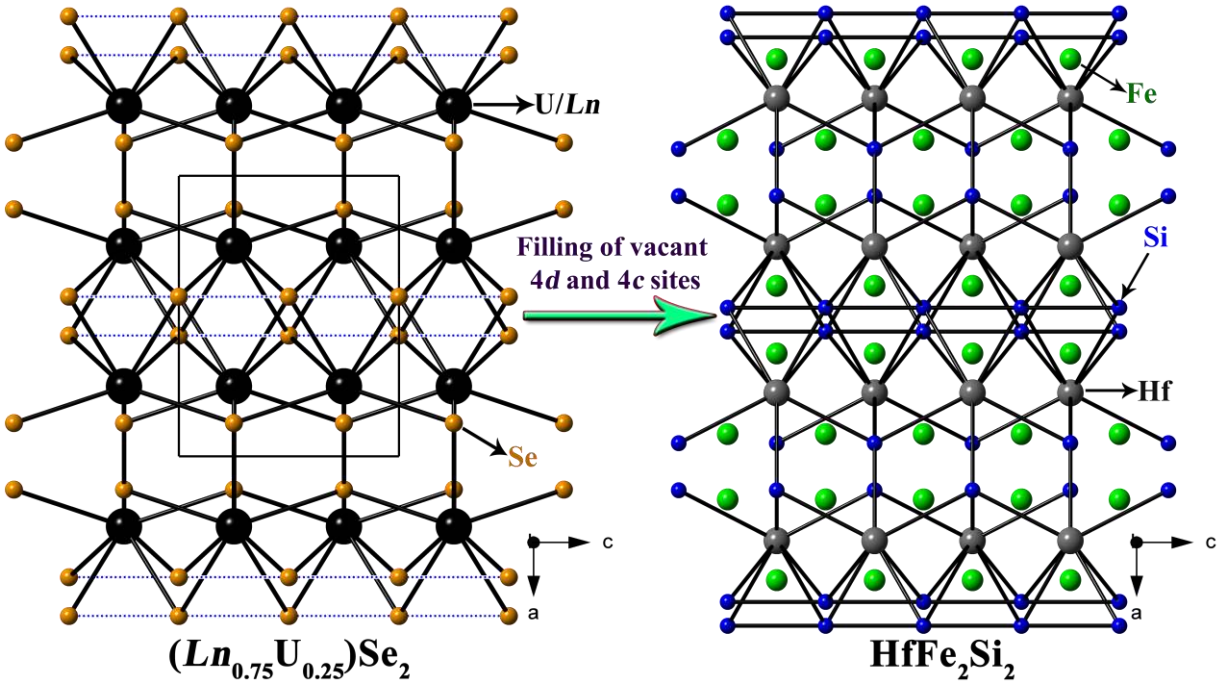
U/Ln
Se
c
a
Filling of vacant
4d and 4c sites
Fe
Si
Hf
c
a
(Ln0.75U0.25)Se2
HfFe2Si2

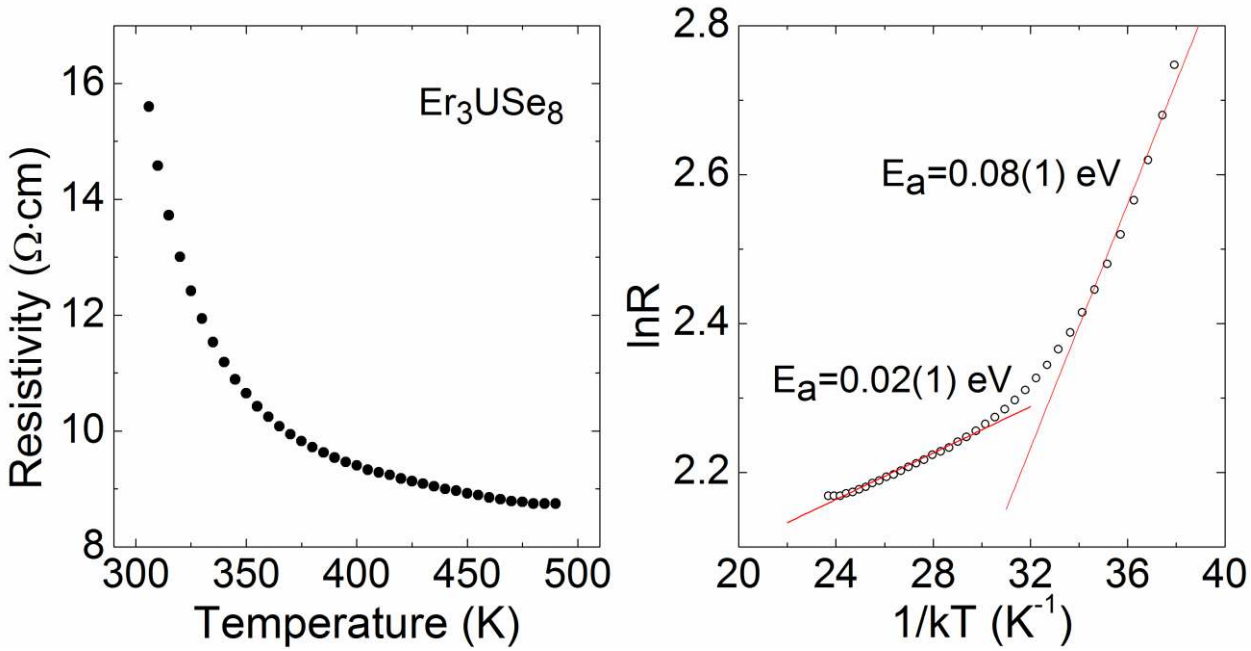
Er3USe8
Resistivity (Ω·cm)
Temperature (K)
16
14
12
10
8
300
350
400
450
500
lnR
1/kT (K-1)
Ea=0.08(1) eV
Ea=0.02(1) eV
2.8
2.6
2.4
2.2
20
24
28
32
36
40

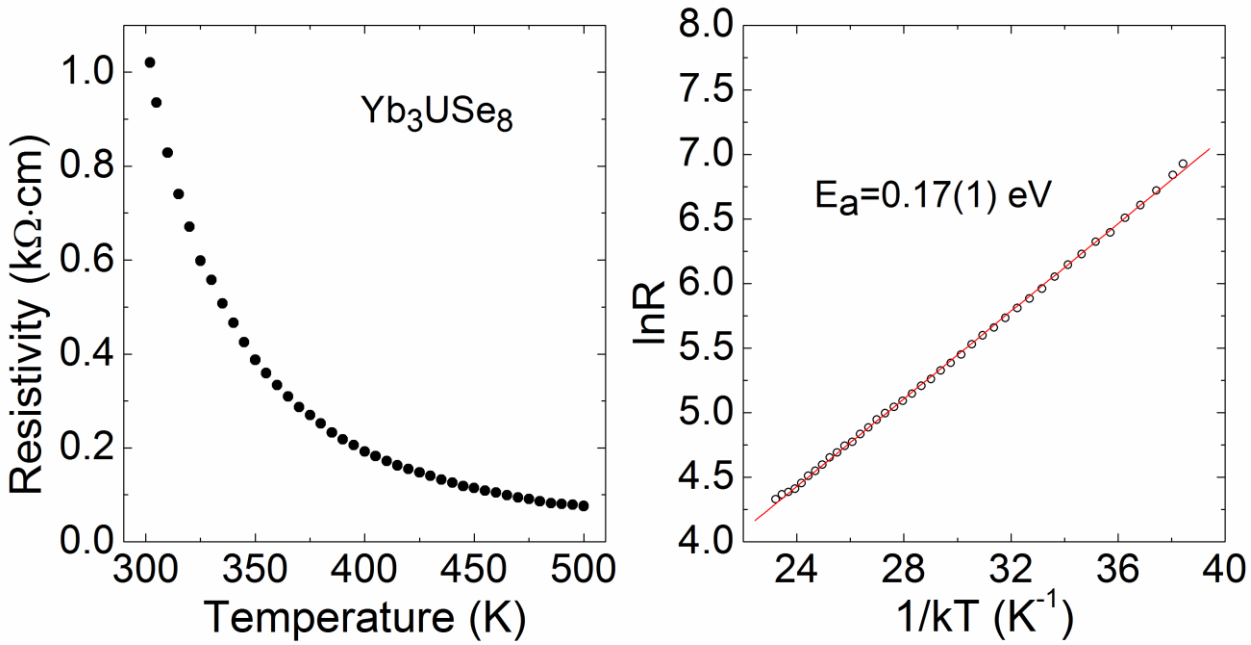
Yb3USe8
Resistivity (kΩ·cm)
Temperature (K)
1.0
0.8
0.6
0.4
0.2
0.0
300
350
400
450
500
Ea=0.17(1) eV
lnR
1/kT (K-1)
8.0
7.5
7.0
6.5
6.0
5.5
5.0
4.5
4.0
24
28
32
36
40

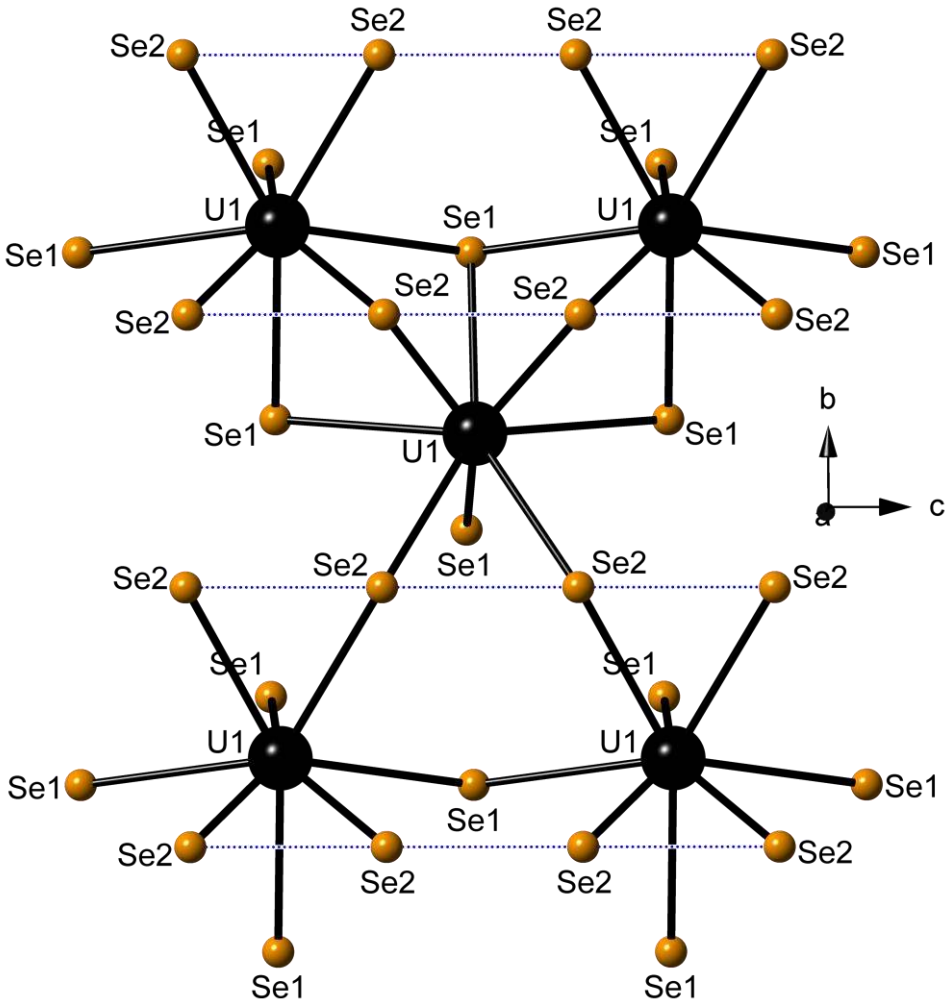
Se2
Se2
Se2
Se2
Se1
Se1
U1
Se1
U1
Se1
Se1
Se2
Se2
Se2
Se2
Se1
U1
Se1
b
c
a
Se2
Se2
Se1
Se2
Se2
Se1
Se1
U1
U1
Se1
Se1
Se2
Se2
Se2
Se2
Se1
Se1

Local coordination environment of (*Ln*/U) atoms in the Ln_3USe_8 (*Ln* = Er, Yb) structure.